RSC Advances

PAPER

View Article Online
View Journal | View Issue

Cite this: *RSC Adv.*, 2017, **7**, 20502

Tyrosinase mediated oxidative functionalization in the synthesis of DOPA-derived peptidomimetics with anti-Parkinson activity†

Bruno M. Bizzarri,[a] Alessandro Martini,[b] Francesco Serafini,[a] Daniela Aversa,[b] Davide Piccinino,[a] Lorenzo Botta,[a] Nicola Berretta,[b] Ezia Guatteo[bc] and Raffaele Saladino *[a]

DOPA-derived peptidomimetics are an attractive therapeutic tool for the treatment of Parkinson's disease. Compounds with unusual O–C and N–C covalent bonds between amino acids have been prepared by selective oxidative functionalization of tyrosine residues with tyrosinase from *Agaricus bisporus*. The reaction proceeded through a Michael-like nucleophilic addition of amino acids on the DOPA quinone intermediate initially produced by tyrosinase oxidation. The reaction was effective under heterogeneous conditions by immobilization of tyrosinase on multi walled carbon nanotubes (MWCNTs). The anti-Parkinson activity of novel DOPA-derived peptidomimetics was evaluated by electrophysiological techniques on individual dopaminergic neurons in rat *ex vivo* midbrain slices. Gly-*N*-C-DOPA and Val-*N*-C-DOPA-derived peptidomimetics inhibited neuronal firing and evoked outward currents *via* activation of the D2 receptors in most dopamine-sensitive neurons. In a subset of neurons which displayed low dopamine sensitivity, Gly-*N*-C-DOPA also caused significative effects.

Received 21st March 2017
Accepted 30th March 2017

DOI: 10.1039/c7ra03326e

rsc.li/rsc-advances

Introduction

Peptidomimetics are modified peptides which might have optimal bioavailability and biological activity.[1,2] The modifications usually involve *N*-alkylation, Cα-substitution, Cα and N-replacement, heterocyclic generation, and backbone or side-chain transformations.[3] Among peptidomimetics, DOPA derivatives are of interest in the therapy of the Parkinson disease (PD).[4] PD is one of the most important neurodegenerative disorders, characterized by dopamine (DA) neuron loss in the substantia nigra pars compacta (SNpc) and depletion of DA content in the dorsal striatum, which causes tremors at rest, muscle rigidity, akinesia (or bradykinesia) and postural instability.[5]

DOPA-containing peptides penetrate the blood brain barrier (BBB) by the aid of specific peptide-mediated carrier transport systems (PMCTS),[6] restoring adequate DA concentration in the surviving dopaminergic (DAergic) neurons.[7] They also preserve DOPA from the occurrence of fast metabolic decarboxylation, avoiding the peripheral DA-related side effects (cardiac arrhythmias, vomiting and hypotension).[8] DOPA peptides showed bioavailability and anti-PD activity higher than DOPA.[9]

The main synthetic pathway for the preparation of DOPA peptides is the solid state procedure.[10] This synthesis often requires tedious and long-time protecting/de-protecting steps, with intrinsic low selectivity.[11] As an alternative, procedures based on the oxidative side chain modification of amino acids have been applied.[12] The synthesis of DOPA-containing peptides by selective oxidation of tyrosine residues with tyrosinase from *Agaricus bisporus* was reported.[13,14] Tyrosinase (monophenol, *o*-diphenol: oxidoreductase, E.C. 1.14.18.1) is a metalloprotein able to activate di-oxygen for the conversion of tyrosine to DOPA (creolase or monophenolase activity) and to DOPA quinone (catecholase or diphenolase activity, respectively).[15–18]

The replacement of the natural amide bond in peptides with unusual covalent linkages is a general strategy to improve the stability and activity of the molecule.[19] We recently reported the synthesis of DOPA-derived peptidomimetics with stable O–C and N–C covalent bonds by oxidative functionalization of tyrosine with 2-iodoxybenzoic acid (IBX),[20] that is a biomimetic system of tyrosinase. The reaction proceeded through a Michael-like 1,4-addition of oxygen and nitrogen centred α-amino acids to reactive DOPA *ortho*-quinone intermediate.[21] DOPA-derived peptidomimetics containing glycine residues showed the highest antioxidant effect in the 2,2-diphenyl picrylhydrazyl (DPPH) test, while valine derivatives were the most active compounds in the comet assay in L5178Y (TK±) mouse lymphoma cells.[20]

[a]*Department of Ecological and Biological Sciences (DEB), University of Tuscia, Via S Camillo de Lellis, 01100 Viterbo, Italy. E-mail: saladino@unitus.it*

[b]*Laboratory of Experimental Neurology, Fondazione Santa Lucia IRCCS, Via del Fosso di Fiorano 64, 00143 Roma, Italy*

[c]*University of Naples Parthenope, Via Medina 40, 80133 Napoli, Italy*

† Electronic supplementary information (ESI) available: ^{1}H and ^{13}C NMR spectra of DOPA peptidomimetics **2–9**. See DOI: 10.1039/c7ra03326e

The role of the oxidative stress in PD has been debated and reviewed.[22] Data suggested that the oxidative damage by active radical species might contribute to the cascade of events leading to degeneration of DAergic neurons.[23]

We report here that tyrosinase can be directly applied for the nucleophilic oxidative functionalization of tyrosine residues to yield DOPA-derived peptidomimetics bearing stable O–C and N–C bonds and characterized by antioxidant and anti-Parkinson activities. The reaction was effective under heterogeneous conditions after immobilization of tyrosinase on multi walled carbon nanotubes (MWCNTs). The main advantages of heterogeneous catalysis derive from the easy product isolation, high enzyme loading and recyclability, thus minimizing the cost of the processes.[24] The anti-Parkinson activity of novel DOPA-derived peptidomimetics was evaluated by electrophysiological recordings on individual dopaminergic neurons in rat *ex vivo* midbrain slices, based on the ability of novel DOPA-derived peptidomimetics to reproduce the effects of DA and DOPA observed on the DAergic neurons in physiological conditions. Indeed, the low content of DA in the basal ganglia nuclei occurring in PD is currently mainly treated with DOPA which is converted to DA by the aromatic amino acid decarboxylase enzyme. Therefore, the efficacy of potential anti-PD drugs should be expressed through their ability to mimic DA/DOPA effects.

Results and discussion

Synthesis of DOPA-derived peptidomimetics under homogeneous conditions

The tyrosine derivative Boc-Tyr-OMe (BTO) **1** protected at both the amino moiety (as *tert*-butoxycarbonyl; Boc, green) and carboxylic group (as methyl ester; cyano) was used as starting material. Reactions were designed according to the general procedure previously applied with IBX and are generalized in Scheme 1.

Briefly, the oxidation of BTO **1** (20 mg, 0.068 mmol) with tyrosinase from *Agaricus bisporus* (600 UA) was performed in the presence of the appropriate α-amino acid derivative (0.68 mmol) in phosphate buffer solution (PBS; pH 7) and EtOH (from 9 : 1 v/v to 1 : 9 v/v PBS/EtOH ratio, respectively) at 25 °C, followed by the reduction step with $Na_2S_2O_4$. EtOH showed a complete miscibility and high compatibility with PBS in various enzymatic reactions.[25] Initially, glycine methyl ester

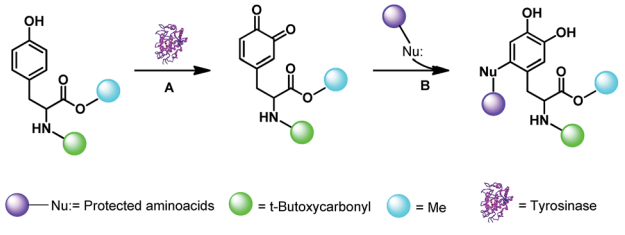

Scheme 1 General reactivity scheme of Boc-Tyr-OMe (BTO) **1** with α-amino acids in the presence of tyrosinase from *Agaricus bisporus*. Step A: oxidation of tyrosine to DOPA-quinone. Step B: Michael-like 1-4-addition of α-amino acids on the DOPA-quinone intermediate, followed by the reduction step with $Na_2S_2O_4$.

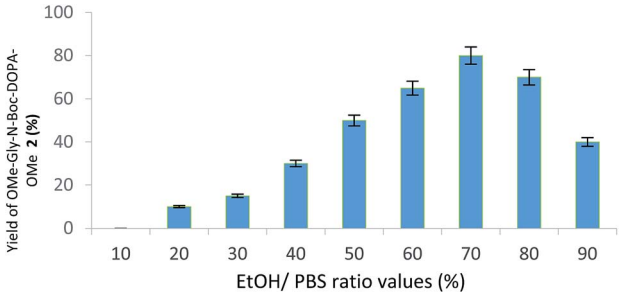

Fig. 1 Yield (%) of OMe-Gly-*N*-Boc-DOPA-OMe **2** during the oxidation of BTO **1** with tyrosinase from *Agaricus bisporus* in the presence of NH_2-Gly-OMe at different EtOH/PBS ratio values. Experiments were conducted on triplicate.

(NH_2-Gly-OMe) was used as nitrogen centred nucleophile for the addition on the reactive DOPA *ortho*-quinone intermediate. DOPA-derived peptidomimetic OMe-Gly-*N*-Boc-DOPA-OMe **2** was obtained in the highest yield (87%) in the presence of PBS/EtOH 3 : 7 v/v after 24 h, besides to unreacted BTO (Fig. 1; Scheme 2, pathway A; Table 1).

The oxidative functionalization of BTO **1** was then repeated using *N*-Boc-glycine (Boc-Gly-COOH) as oxygen centred nucleophile under optimal conditions, to yield *N*-Boc-Gly-*N*-Boc-DOPA-OMe **3** in 80% yield (Table 1, entry 3), besides to residual BTO (Scheme 2, pathway B). To evaluate the generality of the transformation, we used the more hindered amino acids NH_2-Val-OMe and *N*-Boc-Val-COOH as nucleophiles.

The corresponding DOPA-derived peptidomimetics OMe-Val-*N*-Boc-DOPA-OMe **4** and *N*-Boc-Val-*N*-Boc-DOPA-OMe **5** were obtained in 77% and 74% yield, respectively (Table 1, entries 2

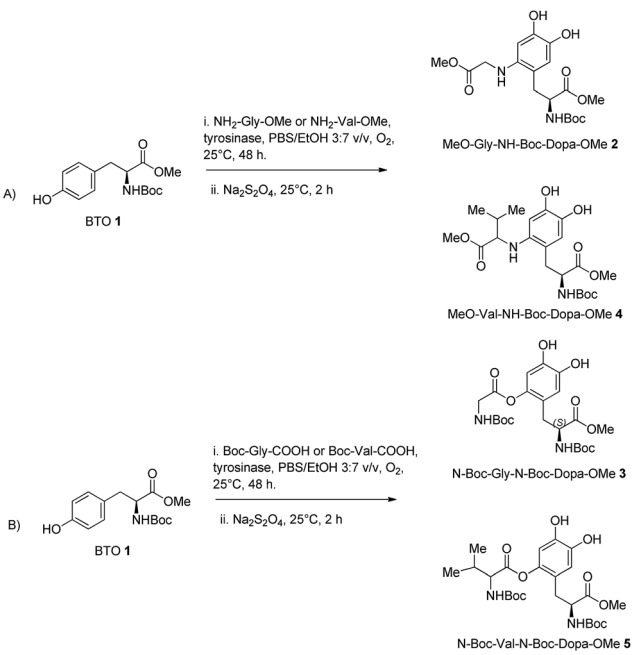

Scheme 2 Synthesis of DOPA-derived peptidomimetics **2**–**5** by oxidative functionalization of BTO **1** with tyrosinase from *Agaricus bisporus* in the presence of glycine and valine nucleophiles.

Table 1 Synthesis of O–C and N–C bonded DOPA-derived peptidomimetics under homogeneous and heterogeneous conditions

Entry	Nucleophile	Catalyst	Product	Yield (%)
1	NH_2-Gly-OMe	Tyrisonase[a]	OMe-Gly-*N*-Boc-DOPA-OMe **2**	87
2	*N*-Boc-Gly-COOH	Tyrosinase	*N*-Boc-Gly-*N*-Boc-DOPA-OMe **3**	80
3	NH_2-Val-OMe	Tyrosinase[a]	OMe-Val-*N*-Boc-DOPA-OMe **4**	77
4	*N*-Boc-Val-COOH	Tyrosinase	*N*-Boc-Val-*N*-Boc-DOPA-OMe **5**	74
5	NH_2-Gly-OMe	Tyr/MWCNT[b]	OMe-Gly-*N*-Boc-DOPA-OMe **2**	85
6	*N*-Boc-Gly-COOH	Tyr/MWCNT	*N*-Boc-Gly-*N*-Boc-DOPA-OMe **3**	79
7	NH_2-Val-OMe	Tyr/MWCNT[b]	OMe-Val-*N*-Boc-DOPA-OMe **4**	75
8	*N*-Boc-Val-COOH	Tyr/MWCNT	*N*-Boc-Val-*N*-Boc-DOPA-OMe **5**	70
9	NH_2-Gly-OMe	Tyr/MWCNT[c]	OMe-Gly-*N*-Boc-DOPA-OMe **2**	88
10	NH_2-Gly-OMe	Tyr/MWCNT	OMe-Gly-*N*-Boc-DOPA-OMe **2**	85
11	NH_2-Gly-OMe	Tyr/MWCNT	OMe-Gly-*N*-Boc-DOPA-OMe **2**	85
12	NH_2-Gly-OMe	Tyr/MWCNT	OMe-Gly-*N*-Boc-DOPA-OMe **2**	83
13	NH_2-Gly-OMe	Tyr/MWCNT	OMe-Gly-*N*-Boc-DOPA-OMe **2**	81

[a] BTO **1** (20 mg, 0.068 mmol) was treated with tyrosinase from *Agaricus bisporus* (600 UA) and different α-amino acid residues (0.68 mmol) in PBS/EtOH (3 : 7 v/v; mL) at 25 °C for 24 h, followed by the reduction step with $Na_2S_2O_4$. [b] BTO **1** (20 mg, 0.068 mmol) was treated with Tyro/MWCNT (600 UA) and different α-amino acid residues in PBS/EtOH (3 : 7 v/v; 12 mL) at 25 °C for 24 h, followed by the reduction step with $Na_2S_2O_4$. [c] Reusability is expressed as the yield in % of DOPA-derived peptidomimetic **2** obtained by oxidation of BTO **1** with MWCTN/Tyr under optimal conditions.

and 4), besides to residual BTO (Scheme 2, pathways A and B). As a general trend, N-centred nucleophiles were slightly more efficient than the O-centred counterpart. Moreover, glycine nucleophiles were more reactive than valine nucleophiles, probably due to side-chain steric hindrance effects.

Synthesis of DOPA-derived peptidomimetics in heterogeneous conditions

The oxidative functionalization of BTO **1** was then performed using tyrosinase supported on multi-walled carbon nanotubes (MWCNTs) applying the Layer by Layer (LbL) procedure previously developed.[26] Briefly, oxidized MWCNTs[27] were treated with a positively charged poly(diallyldimethylammonium) chloride (PDDA) to facilitate the loading of tyrosinase, that is negatively charged at the operative pH 7. Bovine Serum Albumin (BSA) was used to reduce undesired conformational changes.[28] Glutaraldehyde (GA) increased the reticulation grade and the stability of the system (Fig. 2).[29] The structural characterization and the activity parameters of catalyst MWCNT/tyrosinase/BSA (Tyr/MWCNTs), as well as its application in the synthesis of bioactive catechol derivatives are in ref. 26. The oxidation of BTO **1** (20 mg, 0.068 mmol) with Tyro/MWCNT (600 UA) in PBS/EtOH (7 : 3 v/v, 12 mL) at 25 °C for 24 h in the presence of NH_2-Gly-OMe or *N*-Boc-Gly-COOH (0.68 mmol) afforded compounds **2** and **3** in 85% and 79% yield, respectively (Table 1, entries 5 and 6). In a similar way, the oxidative functionalization of BTO **1** (20 mg, 0.068 mmol) with NH_2-Val-OMe and Boc-Val-COOH (0.68 mmol) afforded compounds **4** and **5** in 75% and 70% yield, respectively (Table 1, entries 7 and 8).

Recycling experiments proceeded with success in the oxidation of compound BTO **1** with NH_2-Gly-OMe as selected nucleophile. As shown in Table 1 (entries 9–13), MWCNT/Tyr was used for at least five catalytic cycles with only a slight decrease of efficiency to give **2**.

Finally, DOPA-derived peptidomimetics **2–5** were deprotected under standard conditions[30] using 6 M hydrochloric acid heating at reflux for 2 h. Gly-*N*-C-DOPA **6** and Val-*N*-C-DOPA **7** were obtained in quantitative yield, while Gly-*O*-C-DOPA **8** and Val-*O*-C-DOPA **9** were isolated in 73% and 68% yield respectively, probably due to the competitive hydrolysis of the novel C–O bond (Scheme 3).

Evaluation of anti-Parkinson activity

Preliminary studies showed that DOPA-derived peptidomimetics **2–5** were characterized by an antioxidant activity higher than that of the corresponding DOPA-containing peptides.[20] On

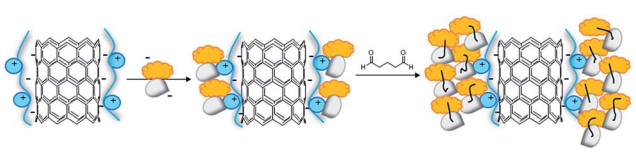

Fig. 2 Loading of tyrosinase (white) on oxidized MWCNTs coated with positively charged poly(diallyldimethylammonium) chloride PDDA (blue). Bovine Serum Albumin (BSA; orange) was used to reduce undesired tyrosinase conformational changes and glutaraldehyde (GA black lines) to increase the reticulation grade and the stability of the overall system.

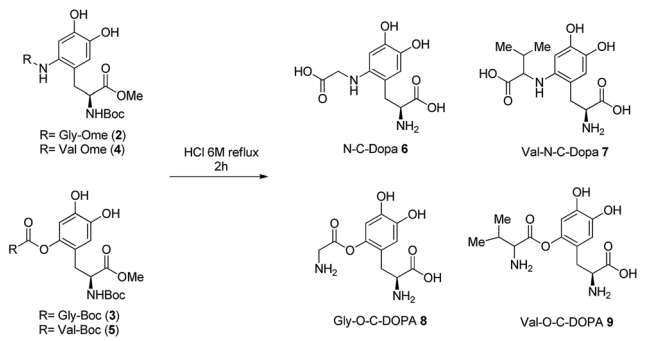

Scheme 3 Deprotection of DOPA-derived peptidomimetics **2–5** to afford Gly-*N*-C-DOPA **6**, Val-*N*-C-DOPA **7**, Gly-*O*-C-DOPA **8**, and Val-*O*-C-DOPA **9**.

the basis of these data, we decided to evaluate the anti-PD effect of peptidomimetics **2–9** (protected and deprotected forms) on DAergic neurons. Since PD is characterized by low content of DA in the basal ganglia nuclei, potential anti-PD drugs should mimic the effects of DA and/or DOPA. Thus, the activity of DOPA-derived peptidomimetics **2–9** was evaluated by measuring the effects on single neuron firing/membrane currents in comparison to those evoked by exogenous DA/DOPA applied to DAergic neurons of the rat substantia nigra pars compacta (SNpc).[31] Simultaneous neuronal firing of a large population of neurons located in the SNpc was recorded by multi electrode array (MEA). Spontaneously active neurons were firstly challenged with DA (30 μM, 2 min, Fig. 3A) and only neurons that were inhibited by DA (>15% spontaneous firing inhibition);[32] were considered in the present study. Similarly, the effect of the DOPA-derived peptidomimetics **2–9** was evaluated in those DA sensitive neurons, which responded to drug perfusion with at least a 15% change in firing rate.

We recorded 39 neurons inhibited by DA, and in 33 of them the application of Gly-*N*-C-DOPA **6**, (300 μM) caused a slow onset firing inhibition that was completely reversed by the D2 receptor antagonist sulpiride (10 μM; Fig. 3, panels A and B). The extent of firing inhibition by Gly-*N*-C-DOPA **6** paralleled that of DA. Indeed, the effect of Gly-*N*-C-DOPA **6** was more pronounced ($P = 0.00014$; Fig. 3, panel B) in those DA-sensitive neurons that were strongly inhibited by DA (74.66 ± 7.07%, $N = 17$), compared to those ($P = 0.041$; Fig. 3, panel C) inhibited by DA by a lesser extent (35.96 ± 9.03%, $N = 16$). In 6 out of the 39 SNpc DA neurons, Gly-*N*-C-DOPA **6** (300 μM) did not cause firing inhibition (<15%), although they responded to DA with 26.73 ± 10.88% firing inhibition (data not shown). To further investigate the neuronal response to Gly-*N*-C-DOPA **6** we performed voltage clamp experiments from single DA neurons. We found that application of Gly-*N*-C-DOPA **6** activated a slowly developing outward current of about 60 pA in 1 out of 3 DAergic neurons tested (Fig. 3, panel F). This current was completely blocked by the D2 receptor antagonist sulpiride. In the remaining 2 neurons Gly-*N*-C-DOPA **6** was ineffective. By contrast, the protected form OMe-Gly-*N*-Boc-DOPA-OMe **2** (300 μM) did not cause significant modifications of firing activity of DAergic neurons ($N = 40$, $P = 0.36744$; Fig. 3D and E). These data suggested that the deprotection of **2** was a key step for the appearance of DA-like effects in the subpopulation of DAergic neurons. Since Gly-*N*-C-DOPA **6** cannot release DA due to the stable N–C linkage between the amino acid residues, the observed activity could be explained by the direct interaction with D2 receptors in the extracellular environment.

We then tested the DA/DOPA-like effects of OMe-Val-*N*-Boc-DOPA-OMe **4** and Val-*N*-C-DOPA **7**, respectively. We recorded 15 SNpc neurons inhibited by DA, and in 12 of these neurons the application of Val-*N*-C-DOPA **7** (300 μM) caused a pronounced ($P = 0.000001$) firing inhibition. This inhibition was completely reversed by the D2 receptor antagonist sulpiride (10 μM; Fig. 4, panels A and B). In these experiments, 3 out of 15 DAergic neurons were insensitive to Val-*N*-C-DOPA **7**, (300 μM; <15%) despite they displayed an inhibition by DA of 84.34 ± 0.79% (data not shown). In a large set of population (53 out of

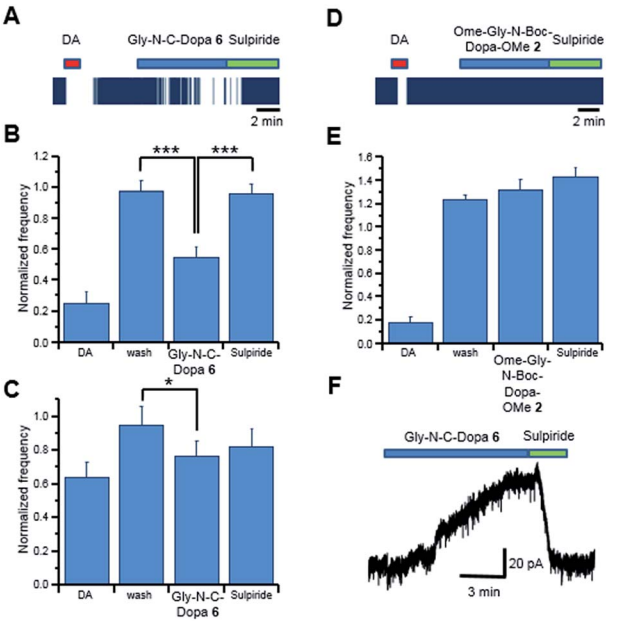

Fig. 3 Acute effects of Gly-*N*-C-DOPA **6** on SNpc DA neurons. (A) Raster plot of the spontaneous firing recorded with MEA form a single SNpc DA neuron. DA (30 μM) robustly inhibited firing and, after complete washout of the DA effect, Gly-*N*-C-DOPA **6** (300 μM) caused a similar slow-onset inhibition of firing. Application of sulpiride (10 μM) completely reversed Gly-*N*-C-DOPA **6**-mediated firing inhibition to control value. (B) Group data showing mean firing frequencies, normalized to control value, in 17 SNpc DA neurons during application of DA, washout, Gly-*N*-C-DOPA **6** and sulpiride. Note that firing frequency returned to control values both after DA washout and in the presence of sulpiride. (C) Group data showing mean firing frequencies, normalized to control value, during application of DA, washout, Gly-*N*-C-DOPA **6** and sulpiride, in 16 SNpc DA neurons poorly sensitive to DA. Similarly, to DA, also Gly-*N*-C-DOPA **6** exerted only a limited inhibition of firing. Sulpiride effect was minimal. (D) Raster plot of the spontaneous firing recorded with MEA form a single SNpc DA neuron. DA (30 μM) robustly inhibited firing and, after complete washout of the DA effect, the protected form OMe-Gly-*N*-Boc-DOPA-OMe **2** (300 μM) did not affect neuronal firing. No effect was also evident in sulpiride (10 μM). (E) Group data showing mean firing frequencies, normalized to control value, in 40 SNpc DA neurons during application of DA, washout, OMe-Gly-*N*-Boc-DOPA-OMe **2** and sulpiride. Note that no significant change of firing frequency was observed from DA washout. (F) Voltage clamp recording ($V_h = -60$ mV) from a single SNpc DA neuron showing Gly-*N*-C-DOPA **6** activated an outward current that was completely blocked by sulpiride. Experiments were conducted on triplicate.

62) of SNpc neurons inhibited by DA OMe-Val-*N*-Boc-DOPA-OMe **4** (300 μM) caused marked firing inhibition (Fig. 4, panels C and D), however, differently from Val-*N*-C-DOPA **7**, the cellular inhibition seemed to be unspecific, as it was not reversed by sulpiride.

These results were further confirmed by patch-clamp recordings. In the example trace of Fig. 4 (panel E), OMe-Val-*N*-Boc-DOPA-OMe **4** caused an outward current that was insensitive to sulpiride. By contrast, the outward current was completely blocked by the K_{ATP} channel blocker tolbutamide (100 μM). These data suggested that OMe-Val-*N*-Boc-DOPA-OMe **4** caused firing inhibition through a mechanism other than D2

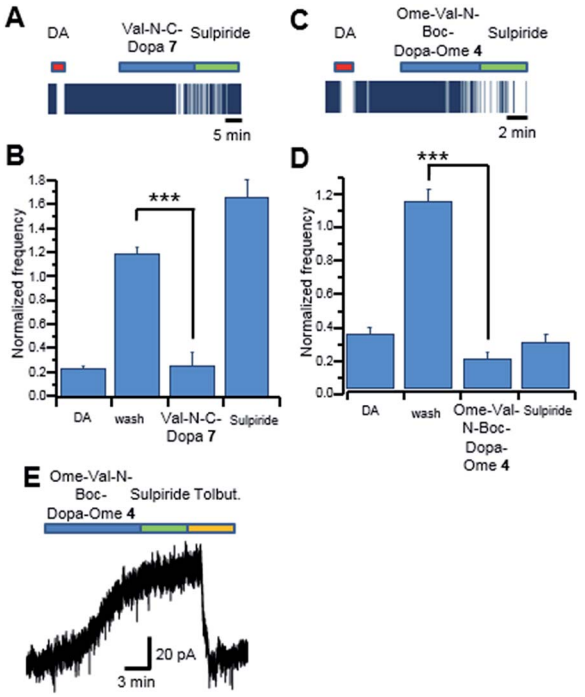

Fig. 4 Acute effect of Val-*N*-C-DOPA **7** and OMe-Val-*N*-Boc-DOPA-OMe **4** on rat SNpc DAergic neurons. (A) Raster plot of the spontaneous firing recorded with MEA. DA (30 μM) strongly inhibited firing and, after complete washout, the deprotected form of Val-*N*-C-DOPA **7** (300 μM) caused a slow-onset inhibition of firing, which was reversed by sulpiride (10 μM). (B) Group data showing mean firing frequencies in the presence of DA, washout, deprotected Val-*N*-C-DOPA **7** and sulpiride, in 12 SNpc DA neurons. (C) Raster plot of the spontaneous firing recorded with MEA. DA (30 μM) strongly inhibited firing and, after complete washout, OMe-Val-*N*-Boc-DOPA-OMe **4** (300 μM) caused a slow-onset inhibition of firing. However, application of sulpiride (10 μM) did not reverse OMe-Val-*N*-Boc-DOPA-OMe **4** effect. (D) Group data showing mean firing frequencies in the presence of DA, washout, L-DOPA Val Ome and sulpiride, in 53 SNpc DA neurons. (E) Patch clamp recording of membrane current ($V_h = -60$ mV) of a single SNpc DA neuron. Application of OMe-Val-*N*-Boc-DOPA-OMe **4** (300 μM) activated an outward current that was insensitive to sulpiride and fully blocked by tolbutamide (100 μM). Experiments were conducted on triplicate.

receptor stimulation, possibly involving a drop in intracellular ATP content, which causes K_{ATP} channel opening. In alternative, the direct action on K_{ATP} channels in SNpc DAergic neurons cannot be completely ruled out.[33]

In 9 out of the 62 SNpc DAergic neurons OMe-Val-*N*-Boc-DOPA-OMe **4** (300 μM) did not cause firing inhibition (<15%), although they responded to DA with 85.78 ± 6.49% firing inhibition (data not shown). Note that O–C DOPA-derived peptidomimetics **3**, **5**, **8** and **9**, were not active under the same experimental conditions, suggesting a structure activity relationships between the inhibition of neuronal firing and evoked outward currents of DAergic neurons and the type of covalent bond. Future experiments will address the possible mechanisms underlying Gly-*N*-C-DOPA **6** and Val-*N*-C-DOPA **7** mediated activation of D2 receptors, and their ability to enter DAergic neurons.

Experimental

Materials

Mushroom tyrosinase from *Agaricus bisporus* (Tyr), multi-walled carbon nanotubes (MWCNTs), L-tyrosine, bovine serum albumin (BSA), glutaraldehyde (GA), poly-diallyldimethylammonium chloride (PDDA), sodium sulfate anhydrous (Na_2SO_4), Boc-tyrosine-OMe, amino acids differently protected and organic solvents were purchased from Sigma-Aldrich. All spectrophotometric measurements were made with a Varian Cary50 UV-Vis spectrophotometer equipped with a Peltier thermostatted single cell holder. ^{1}H and ^{13}C NMR spectra were recorded on a Bruker (400 MHz) spectrometer. Mass spectra were recorded on a VG 70/250S spectrometer with an electron beam of 70 eV. All experiments were done in triplicate using native and immobilized tyrosinase in EtOH/buffer system and in H_2O medium. Sodium phosphate [(PBS) 0.1 M, pH 7.0] was used as the buffer solution.

Preparation of catalyst MWCNT/Tyr

MWCNT/Tyr was prepared as previously reported.[26] Briefly, PDDA coated MWCNTs in PBS were treated with a mixture of Tyr (0.2 mg) and BSA (0.6 mg) for 30 minutes. Glutaraldehyde (GA, 2.5%) was added to reach a final volume of 800 μL and the mixture was shaken at 25 °C for 30 min and at 4 °C overnight. The excess enzyme and GA were removed by centrifugation (4000g × 20 min) and the surnatant was used for the calculation of activity parameters. The catalyst was finally treated with 1.5 mL TRIS–HCl 0.1 M pH 7.2 by shaking for 1 h at 4 °C and centrifuged. MWCNT/Tyr was washed several times with PBS in order to ensure the complete removal of unbounded Tyr (as evaluated by the Bradford method).

Activity data

The activity of native and immobilized Tyr was determined by measuring the oxidation of L-tyrosine. The reaction was started by adding L-tyrosine to the solution of Tyr or MWCNT/Tyr in PBS under magnetic stirring. The initial rates were measured as linear increase in optical density at 475 nm, due to dopachrome formation. One unit of enzyme activity was defined as the increase in absorbance of 0.001 per minute at pH 7, 25 °C in a 3.0 mL reaction cuvette containing 0.83 mM of L-tyrosine and 67 mM of PBS pH 7.0. The activity was expressed as activity unit per milligram of support:

$$\text{Activity (U mg}^{-1}) = U_x/W_{\text{support}}$$

where U_x is the activity of the immobilized enzyme assayed by dopachrome method. The activity yield represents the % of the ratio of activity of the immobilized enzyme to the total units of native enzyme used:

$$\text{Activity yield (\%)} = [U_x/(U_a - U_r)] \times 100$$

where U_a is the total activity of enzyme (unit) added in the solution and U_r is the activity of the residual Tyr (unit) evaluated

by dopachrome method in the washing solutions. The immobilization yield is defined as:

$$\text{Immobilization yield (\%)} = [(U_a - U_r)/U_a] \times 100$$

General procedure for preparation of DOPA-derived peptidomimetics

BTO **1** (0.068 mmol) was dissolved in 12 mL of EtOH/PBS v/v, then amino acid (0.68 mmol) and tyrosinase from *Agaricus bisporus* or Tyr/MWCNT (600 UA) were added. The reaction mixture was stirred at 25 °C for 24 h. The reaction was monitored by thin layer chromatography (TLC, *n*-hexane/EtOAc = 2.0 : 1.0). After the disappearance of substrate, the reaction mixture was treated with 2 mL of H_2O and 2.0 eq. of $Na_2S_2O_4$ stirring for 15 min. Then was added 2 mL of saturated solution of $NaHCO_3$ and stirring for 30 min. The mixture was extracted several time with AcOEt and separated from H_2O. The organic layer were collected dried with Na_2SO_4 and concentrated under reduced pressure. The crude product was purified by flash-chromatography. Compounds Gly-*N*-C-DOPA **6**, Val-*N*-C-DOPA **7**, Gly-*O*-C-DOPA **8**, and Val-*O*-C-DOPA **9** were obtained from compounds **2**, **3**, **4** and **5** respectively using an aqueous solution of HCL 6 M for 2 h at reflux. The crude was then concentrated under reduced pressure and washed with hexane to yield the desired products.

Spectroscopic data

OMe-Gly-*N*-Boc-DOPA-OMe (2). Oil ^{1}H NMR (400 MHz, $CDCl_3$): δ_H (ppm) = 1.44 (9H, s, 3 × CH_3), 2.90–3.10 (2H, m, CH_2), 3.74 (3H, s, OCH_3), 3.93 (2H, s, CH_2), 4.11 (3H, s, OCH_3), 4.62–5.14 (1H, m, CH), 7.24 (1H, s, CH), 7.42 (1H, s, CH) ^{13}C NMR (100 MHz, $CDCl_3$): δ_H (ppm) = 28.04 (3 × CH_3), 32.21 (CH_2), 42.89 (CH_2), 52.47 (OCH_3), 52.59 (OCH_3), 56.59 (CH), 80.48 (–C≡), 113.58 (Car), 117.31 (Car), 119.31 (Car), 141.44 (Car), 144.76 (Car), 146.56 (Car), 158.32 (C=O), 171.90 (C=O), 172.64 (C=O). MS (EI): *m*/*z* 399; elemental analysis calcd: C, 54.26; H, 6.58; N, 7.03; O, 32.13 elemental analysis found: C, 54.25; H, 6.59; N, 7.08; O, 32.13.

***N*-Boc-Gly-*N*-Boc-DOPA-OMe (3).** Oil ^{1}H NMR (400 MHz, $CDCl_3$): δ_H (ppm) = 1.28 (9H, s, 3 × CH_3), 1.44 (9H, s, 3 × CH_3), 2.97–3.00 (2H, m, CH_2), 3.74 (3H, s, OCH_3), 3.94 (2H, s, CH_2), 4.62–5.14 (1H, m, CH), 7.24 (1H, s, CH), 7.42 (1H, s, CH). ^{13}C NMR (100 MHz, $CDCl_3$): δ_H (ppm) = 28.08 (3 × CH_3), 28.70 (3 × CH_3), 32.47 (CH_2), 42.89 (CH_2), 52.47 (OCH_3), 55.79 (CH), 79.53 (–C≡), 80.48 (–C≡), 113.58 (Car), 117.31 (Car), 119.31 (Car), 141.44 (Car), 144.76 (Car), 146.56 (Car), 155.80 (C=O), 158.32 (C=O), 171.90 (C=O), 172.64 (C=O). MS (EI): *m*/*z* 485; elemental analysis calcd: C, 54.54; H, 6.66; N, 5.78; O, 33.02 elemental analysis found: C, 54.51; H, 6.62; N, 5.73; O, 33.01.

OMe-Val-*N*-Boc-DOPA-OMe (4). Oil ^{1}H NMR (400 MHz, $CDCl_3$): δ_H (ppm) = 0.89 (6H, d, 2 × CH_3) J = 4, 1.32 (9H, s, 3 × CH_3), 2.90–3.10 (3H, m, CH, CH_2), 3.74 (3H, s, OCH_3), 3.76–3.83 (1H, m, CH), 3.81 (3H, s, OCH_3), 4.49–5.10 (1H, m, CH), 7.49 (2H, s, 2 × CH) ^{13}C NMR (100 MHz, $CDCl_3$): δ_H (ppm) = 19.25 (2 × CH_3), 28.04 (3 × CH_3), 30.63 (CH), 32.21 (CH_2), 52.47 (OCH_3), 52.59 (OCH_3), 55.81 (CH), 74.30 (CH), 80.48 (–C≡), 113.58 (Car), 117.31 (Car), 119.31 (Car), 142.34 (Car), 144.76 (Car), 146.56 (Car), 158.32 (C=O), 171.90 (C=O), 172.64 (C=O). MS (EI): *m*/*z* 441; elemental analysis calcd: C, 57.26; H, 7.32; N, 6.36; O, 29.06 elemental analysis found: C, 57.23; H, 7.31; N, 6.36; O, 29.05.

***N*-Boc-Val-*N*-Boc-DOPA-OMe (5).** Oil ^{1}H NMR (400 MHz, $CDCl_3$): δ_H (ppm) = 0.89–0.98 (6H, d, 2 × CH_3) J = 4, 1.07(9H, s, 3 × CH_3), 1.30 (9H, s, 3 × CH_3), 2.96–3.03 (3H, m, CH, CH_2), 3.74 (3H, s, OCH_3), 3.74–3.85 (1H, m, CH), 4.52–5.14 (1H, m, CH), 7.49 (2H, s, 2 × CH) ^{13}C NMR (100 MHz, $CDCl_3$): δ_H (ppm) = 18.90 (2 × CH_3), 28.08 (3 × CH_3), 28.70 (3 × CH_3), 30.41 (CH), 32.47 (CH_2), 52.47 (OCH_3), 55.79 (CH), 62.71 (CH), 79.53 (–C≡), 80.48 (–C≡), 113.58 (Car), 117.31 (Car), 119.31 (Car), 141.44 (Car), 144.76 (Car), 146.56 (Car), 155.80 (C=O), 158.32 (C=O), 171.90 (C=O), 172.64 (C=O). MS (EI): *m*/*z* 527; elemental analysis calcd: C, 57.02; H, 7.27; N, 5.32; O, 30.38 elemental analysis found: C, 57.00; H, 7.23; N, 5.29; O, 30.35.

Gly-*N*-C-DOPA (6). White solid ^{1}H NMR (400 MHz, D_2O): δ_H (ppm) = 2.90–3.08 (2H, m, CH_2), 3.92 (2H, s, CH_2), 4.59–5.15 (1H, m, CH) J = 4, 7.24 (1H, s, CH), 7.42 (1H, s, CH). ^{13}C NMR (100 MHz, D_2O): δ_H (ppm) = 34.70 (CH_2), 46.29 (CH_2), 56.69 (CH), 99.58 (Car), 115.21 (Car), 117.54 (Car), 134.44 (Car), 139.16 (Car), 145.65 (Car), 176.70 (COOH), 182.24 (COOH). MS (EI): *m*/*z* 271.09; elemental analysis calcd: C, 48.89; H, 5.22; N, 10.37; O, 35.52 elemental analysis found: C, 48.86; H, 5.19; N, 10.36; O, 35.53.

Val-*N*-C-DOPA (7). White solid ^{1}H NMR (400 MHz, D_2O): δ_H (ppm) = 0.89 (6H, d, 2 × CH_3) J = 4, 2.34 (1H, m, CH), 2.89–3.10 (2H, m, CH_2), 4.25–4.37 (1H, m, CH), 4.50–5.10 (1H, m, CH), 7.30 (1H, s, CH), 7.50 (1H, s, CH) ^{13}C NMR (100 MHz, D_2O): δ_H (ppm) = 19.25 (2 × CH_3), 30.33 (CH), 34.71 (CH_2), 56.74 (CH), 76.86 (CH), 99.54 (Car), 115.81 (Car), 116.35 (Car), 134.34 (Car), 139.76 (Car), 146.56 (Car), 179.84 (COOH), 180.25 (COOH). MS (EI): *m*/*z* 313.14; elemental analysis calcd: C, 53.84; H, 6.45; N, 8.97; O, 30.74 elemental analysis found C, 53.80; H, 6.50; N, 8.93; O, 30.77.

Gly-*O*-C-DOPA (8). White solid ^{1}H NMR (400 MHz, D_2O): δ_H (ppm) = 2.90–3.10 (2H, m, CH_2), 3.93 (2H, s, CH_2), 4.62–5.14 (1H, m, CH), 7.21 (1H, s, CH), 7.40 (1H, s, CH). ^{13}C NMR (100 MHz, D_2O): δ_H (ppm) = 33.57 (CH_2), 39.89 (CH_2), 56.77 (CH), 107.23 (Car), 110.66 (Car), 119.31 (Car), 127.46 (Car), 145.61 (Car), 146.30 (Car), 168.20 (COOR), 174.24 (COOH). MS (EI): *m*/*z* 271.09; elemental analysis calcd: C, 48.89; H, 5.22; N, 10.37; O, 35.52 elemental analysis found: C, 48.80; H, 5.18; N, 10.42; O, 35.59.

Val-*O*-C-DOPA (9). White solid ^{1}H NMR (400 MHz, D_2O): δ_H (ppm) = 0.80–0.95(6H, d, 2 × CH_3) J = 4, 2.50–2.60 (1H, m, CH), 2.90–3.10 (2H, m, CH_2), 4.11–4.20 (1H, m, CH), 4.50–5.02 (1H, m, CH), 7.45 (2H, s, 2 × CH) ^{13}C NMR (100 MHz, D_2O): δ_H (ppm) = 18.90 (2 × CH_3), 30.43 (CH), 33.57 (CH_2), 57.75 (CH), 59.21 (CH), 111.26 (Car), 117.61 (Car), 120.36 (Car), 143.56 (Car), 146.73 (Car), 146.91 (Car), 168.95 (COOH), 174.14 (COOH). MS (EI): *m*/*z* 313.14; elemental analysis calcd: C, 53.84; H, 6.45; N, 8.97; O, 30.74 elemental analysis found: C, 53.78; H, 6.52; N, 8.94; O, 30.79.

Electrophysiological recordings

Slice preparation for electrophysiology. Preparation of midbrain slices was performed as described previously[34] from Wistar rats (P18–P23, either sex). All experiments were carried

out in accordance with the international guidelines for the ethical use of experimental animals from the EU Directive 2010/63EU, and authorized by the Italian Health Ministry (Art.31, D.Lgs 26/2014; project protocol 91/2014 PR) and by the local Ethical Committee of the Santa Lucia Foundation. Horizontal slices (thickness 250 or 300 μm) containing the substantia nigra pars compacta (SNpc) and the ventral tegmental area (VTA), were cut with in ice-cold modified artificial CSF (ACSF). This solution contained (in mM): 126 NaCl, 2.5 KCl, 1.2 $MgCl_2$, 1.2 NaH_2PO_4, 2.4 $CaCl_2$, 10 glucose, and 24 $NaHCO_3$, 290 mOs L^{-1}, and was gassed with 95% O_2–5% CO_2, pH 7.4. Slices were kept in a holding chamber containing ACSF at 32 °C, gassed with 95% O_2–5% CO_2 for at least 40 min after slicing procedures. After recovery period, one single slice was transferred to the recording chamber.

Multi-electrode assay recordings. Extracellular signals were acquired on a planar multi-electrode array (MEA) device using the MED64 System (Alpha MED Sciences, Osaka, Japan). Horizontal midbrain slices (300 μm) were placed over an 8 × 8 array of planar microelectrodes, each 20 × 20 μm in size, with an interpolar distance of 100 μm (MED-P2105, Alpha MED Sciences, Osaka, Japan) as previously described.[32] Signals were low-cut filtered at 100 Hz and digitized at 100 kHz using Mobius software (Alpha MED Sciences, Osaka, Japan). The fast transients corresponding to spontaneous action potentials were captured off-line and sorted using Spike2 6.0 software (Cambridge Electronic Design Ltd, Cambridge, UK). The basal firing frequency was measured over a period of 3 min, before challenging the slices with a 30 s perfusion of DA 30 μM. The relative change in firing frequency was calculated by the mean frequency during the last few seconds of DA perfusion with respect to the control period. Only cells that were inhibited by DA, with inhibition exceeding 15% of control firing, were considered in the present study.

Whole cell patch clamp recordings in SNpc DAergic neurons. Recordings were performed accordingly to Mercuri *et al.*[34] SNpc DAergic neurons, localized in a region of tightly packed neurons adjacent to the medial terminal nucleus of the accessory optic tract, were identified based on a slow and regular spontaneous firing (1–5 Hz), hyperpolarizing/outward response to dopamine (DA, 30 μM), prominent I_h in response to hyperpolarizing voltage steps (−60 to −120 mV, 20 mV increment, holding potential, V_h, −60 mV)[35] and, in current-clamp mode, a depolarizing sag upon application of negative currents.[36] Patch pipettes (2–5 MΩ) were filled with a solution containing (in mM): K-gluconate (135), $CaCl_2$ (0.1), $MgCl_2$ (2), KCl (10), EGTA (0.75), HEPES (10), Mg_2-ATP (4), and Na_3-GTP (0.3), phosphocreatine-Na_2 (10), pH 7.3, osmolarity 280 mOs L^{-1}.

Conclusions

DOPA-derived peptidomimetics bearing unusual O–C and N–C bonds have been efficiently prepared by a novel tyrosinase mediated oxidative functionalization process, based on the nucleophilic addition of appropriate amino acids on the reactive *ortho*-quinone intermediate of tyrosine residues. The reaction was effective also under heterogeneous conditions using tyrosinase immobilized on multi walled carbon nanotubes. We have found that peptidomimetics Gly-*N*-C-DOPA **6** and Val-*N*-C-DOPA **7**, bearing a stable N–C covalent bond between the amino acid residues displayed DA/DOPA-like effects in the majority of SNpc DAergic neurons. Gly-*N*-C-DOPA **6** and Val-*N*-C-DOPA **7** caused a strong inhibition of firing activity *via* D2 receptor activation, and similarly to DA/DOPA, activated the D2 receptor-mediated outward current that was blocked by the selective D2 receptor antagonist sulpiride. However, in a subpopulation of SNpc DAergic neurons poorly sensitive to DA, Gly-*N*-C-DOPA **6** and Val-*N*-C-DOPA **7** exerted only a mild effects. The reason of this discrepancy among different types of SNpc DAergic neurons remains unknown, even if a different membrane expression of functional aromatic aminoacid transporters can be reasonably involved.[37,38]

Acknowledgements

The FILAS project "MIGLIORA" of Latium Region (Italy) is acknowledged.

Notes and references

1 M. C. Recio, J. Andujar and J. L. Rios, *Curr. Med. Chem.*, 2012, **19**, 2088.
2 B. D. Welch, A. P. Van Demark, A. Heroux, C. P. Hill and M. S. Kay, *Proc. Natl. Acad. Sci. U. S. A.*, 2007, **104**, 16828–16833.
3 L. D. Walensky, A. L. Kung and I. Escher, *Science*, 2004, **305**, 1466–1470.
4 M. Kanazawa, H. Ohba, N. Harada, T. Kakiuchi, S. Muramatsu and H. Tsukada, *J. Nucl. Med.*, 2016, **57**, 303–308.
5 P. M. Abou-Sleiman, M. M. Muqit and N. W. Wood, *Nat. Rev. Neurosci.*, 2006, **7**, 207–219.
6 J. P. Bai and G. L. Amidon, *Pharm. Res.*, 1992, **9**, 969–978.
7 Y. J. Fei, Y. Kanai, S. Nussberger, V. Ganapathy, F. H. Leibach, M. F. Romero, S. K. Singh, W. F. Boron and M. A. Hediger, *Nature*, 1994, **368**, 563–566.
8 K. Miyamoto, T. Shiraga, K. Morita, H. Yamamoto, H. Haga, Y. Taketani, I. Tamai, Y. Sai, A. Tsuji and E. Takeda, *Biochim. Biophys. Acta*, 1996, **1305**, 34–38.
9 H. P. Wang, J.-S. Lee, M.-C. Tsai, H.-H. Lu and W. Hsu, *Bioorg. Med. Chem. Lett.*, 1995, **5**, 2195–2198.
10 J. O'Neill, F. Veitch and T. Wagner-Jauregg, *J. Org. Chem.*, 1956, **21**, 363–364.
11 B. M. Bizzarri, S. Tortolini, L. Rotelli, G. Botta and R. Saladino, *Curr. Med. Chem.*, 2015, **22**, 4138–4165.
12 J. Ueda, T. Ozawa, M. Miyazaki and Y. Fujiwara, *J. Inorg. Biochem.*, 1994, **55**, 123–130.
13 C. F. Lazzaro, M. Crucianelli, F. De Angelis, V. Neri and R. Saladino, *Tetrahedron Lett.*, 2004, **45**, 9237–9240.
14 M. Guazzaroni, M. Pasqualini, G. Botta and R. Saladino, *ChemCatChem*, 2012, **4**, 89–99.
15 G. Botta, M. Delfino, M. Guazzaroni, C. Crestini, S. Onofri and R. Saladino, *ChemPlusChem*, 2013, **78**, 325–330.

16 E. I. Solomon and U. M. Sundaram, *Chem. Rev.*, 1997, **96**, 2563–2606.
17 G. Prota, Tyrosinase, in *Melanins and Melanogenesis*, ed. H. B. Jovanovich, Academic Press, 1992, pp. 34–62.
18 J. Espìn, *Eur. J. Biochem.*, 2000, **267**, 1270–1279.
19 S. M. Miller, R. J. Simon, R. N. Zucherman, J. M. Kerr and W. H. Moos, *Drug Dev. Res.*, 1995, **35**, 20–32.
20 B. M. Bizzarri, C. Pieri, G. Botta, L. Arabuli, P. Mosesso, S. Cinelli, A. Schinoppi and R. Saladino, *RSC Adv.*, 2015, **5**, 60354–60364.
21 M. Jimenez, F. Garcia-Carmona, F. Garcia Canovas, J. L. Iborra, J. A. Lozano and F. Martinez, *Arch. Biochem. Biophys.*, 1984, **235**, 438–448.
22 V. Dias, E. Junn and M. Mouradian, *J. Parkinson's Dis.*, 2013, **3**, 461–491.
23 M. F. Beal, *Ann. Neurol.*, 2005, **58**, 495–505.
24 B. Brena, P. González-Pombo and F. Batista-Viera, *Methods Mol. Biol.*, 2013, **1051**, 15–31.
25 O. Barbosa, R. Torres, C. Ortiz, B. Shuster and A. Fishman, *J. Mol. Microbiol. Biotechnol.*, 2009, **6**, 188–200.
26 G. Botta, B. M. Bizzarri, A. Garozzo, R. Timpanaro, B. Bisignano, D. Amatore, A. T. Palamara, L. Nencioni and R. Saladino, *Bioorg. Med. Chem.*, 2015, **23**, 5345–5351.
27 P. Asuri and S. S. Karajanagi, *Biotechnol. Bioeng.*, 2006, **95**, 804–811.
28 G. B. Broun, Chemically aggregated enzymes, *Methods Enzymol.*, 1976, **263**, 280.
29 C. Satish and J. T. Mohapatra, *Biotechnol. Tech.*, 1994, **8**, 13–16.
30 C. Chan, D. Crich and S. Natarajan, *Tetrahedron Lett.*, 1992, **33**, 3405–3408.
31 N. B. Mercuri, P. Calabresi and G. Bernardi, *J. Life Sci.*, 1992, **51**, 711–718.
32 N. Berretta, G. Bernardi and N. B. Mercuri, *J. Physiol.*, 2010, **588**, 1719–1735.
33 E. Guatteo, M. Federici, A. Siniscalchi, T. Knöpfel, N. B. Mercuri and G. Bernardi, *J. Neurophysiol.*, 1998, **79**, 1239–1245.
34 N. B. Mercuri, A. Bonci, P. Calabresi, A. Stefani and G. Bernardi, *Eur. J. Neurosci.*, 1995, **7**, 462–469.
35 E. Guatteo, A. Yee, J. McKearney, M. L. Cucchiaroni, M. Armogida, N. Berretta, N. B. Mercuri and J. Lipski, *Exp. Neurol.*, 2013, **247**, 582–594.
36 E. Guatteo, F. R. Fusco, P. Giacomini, G. Bernardi and N. B. Mercuri, *J. Neurosci.*, 2000, **15**, 6013–6020.
37 L. Sebastianelli, A. Ledonne, M. C. Marrone, G. Bernardi and N. B. Mercuri, *Exp. Neurol.*, 2008, **212**, 230–233.
38 N. B. Mercuri, P. Calabresi and G. Bernardi, *Br. J. Pharmacol.*, 1990, **100**, 257–260.